International Scholars Journals

African Journal of Infectious Diseases Research ISSN 2756-3340 Vol. 13 (11), pp. 001-014, November, 2026. Available online at www.internationalscholarsjournals.org © International Scholars Journals

Author(s) retain the copyright of this article.

Full Length Research Paper

Preclinical safety assessment of the Ad26.CoV2-S vaccine in male Wistar rats: biochemical and histopathological study following phytotherapeutic preconditioning

Dimitry Moudiongui Mboungou Malanda[1,2,3], Bredin Roch Bissala Nkounkou [1], Archange Michel Emmanuel Mboungou Malonga[1], Paola Candyse Tsimba Lemba [1], Elamette Gnyassiba Balebou [1], Syrlie Marina Osseke [1], Landry Martial Miguel[1]

[1]Faculty of Health Sciences, Marien Ngouabi University, Brazzaville, Republic of the Congo;
[2]Department of Anatomy and Cytopathology, Brazzaville University Hospital, Brazzaville, Republic of the Congo;
[3]Research Unit in Virology and Molecular Biology at the FSSA, Brazzaville, Republic of the Congo.

Abstract

Received June 29, 2026; Revised October 30; Accepted November, 01, 2026; Published xxx

Introduction: COVID-19 led to the development of the Ad26.CoV2-S vaccine, a recombinant adenoviral vector expressing the SARS-CoV-2 spike protein. Despite its demonstrated clinical efficacy, its preclinical safety profile requires further evaluation. Objective: This study aims to analyze the biochemical and histopathological effects of the vaccine in Wistar rats, using a plant extract preconditioning model. Materials and Methods: Twenty male rats were divided into five groups: an unimmunized control, groups pretreated with Immu-C®, G. kola, or Z. officinale followed by immunization, and a vaccinated control. The animals received the treatments for seven days and were then immunized with Ad26.CoV2-S. The parameters studied included transaminases (ALT, AST), creatinine, and histopathological lesions of the liver, lungs, and spleen. Results: The results show irregular variations in transaminases, a generally stable creatinine level, and predominantly pulmonary lesions (alveolar congestion and hemorrhage), with limited hepatic and splenic involvement. Two deaths were observed in the vaccinated group after the second immunization. Conclusion: Immunization with Ad26.CoV2-S is associated with moderate biological changes dominated by inflammatory pulmonary lesions, with relative preservation of hepatic and renal function.

Keywords: Ad26.CoV2-S, Phytotherapeutic preconditioning, Biochemistry, Histopathology, Wistar rat.

INTRODUCTION

Coronavirus disease 2019 (COVID-19), caused by SARS-CoV-2, triggered an unprecedented global health crisis [1]. This led to the rapid development of various vaccine platforms aimed at limiting viral transmission, reducing hospitalizations, and decreasing infection-related mortality [2]. Among the vaccines developed, the Ad26.CoV2-S vaccine is based on a recombinant adenoviral vector of serotype

Corresponding authors: dimitrymboungou@yahoo.fr;

26 expressing the SARS-CoV-2 Spike glycoprotein [3]. Its efficacy in preventing severe forms of COVID-19 has been demonstrated in several studies, and its widespread distribution has contributed to global efforts to control the pandemic [4]. Clinical studies generally report a favorable safety profile. However, as with any biological product, a thorough preclinical safety assessment remains essential to characterize physiological responses and any potential biological effects associated with its administration [5]. Preclinical vaccine safety assessment is a fundamental step in vaccine development [6,7]. It allows for the characterization of the potential effects of vaccine candidates on major organs and biological systems before their large-scale use [6,7,8]. In this context, biochemical investigations allow for the assessment of the functional integrity of organs such as the liver and kidneys, while histopathological analysis is an essential tool for detecting any tissue changes occurring after immunization [7,8,9]. The Wistar rat is widely used as an experimental model in toxicological, immunological, and virological studies due to its sensitivity to biological agents and the reproducibility of its responses [9,10]. The combined evaluation of biochemical and histopathological parameters in this animal model provides essential information for understanding the biological processes associated with the post-immunization response and allows for the characterization of the safety profile of vaccines [10,11]. The Ad26.CoV2-S vaccine has been the subject of numerous clinical investigations; however, data concerning biochemical and histopathological changes in experimental models remain limited [11,12]. Analysis of these parameters is therefore necessary to better understand the biological effects associated with vaccination and to distinguish expected physiological responses from potential tissue alterations [12]. In this context, the present study aims to evaluate the biochemical and histopathological changes observed in Wistar rats after immunization with the recombinant adenoviral vector vaccine Ad26.CoV2-S, in a plant-based preconditioning model.

MATERIALS AND METHODS

Experimental animals, plant extract pretreatment, and immunization

For Garcinia kola Heckel, the extracts were prepared by cold macerating 50 g of seed powder in 500 ml of distilled water with stirring for 72 hours, followed by concentration of the extract using a rotary evaporator. For Zingiber officinale Roscoe, fresh roots were ground and then extracted in cold distilled water for 20 minutes, followed by filtration using a method similar to infusion, with a ratio of 0.2 g to 2.5 ml of solvent.

Twenty male Wistar rats weighing 150–300 g were allocated to five experimental groups. The animals received the test substances orally at the respective doses once daily for seven consecutive days. Except for the negative control group, all animals were subsequently immunized intramuscularly with the Ad26.CoV2-S vaccine, a recombinant, non-replicating human adenovirus serotype 26 (Ad26) vector expressing the SARS-CoV-2 Spike protein [13]. Each immunized rat received 50 µL of vaccine preparation. Based on a vaccine concentration of 5×10^{10} viral particles (vp)/mL, the estimated administered dose was 2.5×10^{9} vp per rat, equivalent to 5% of the reference human dose of 5×10^{10} vp. This dose was selected according to the feasible injection volume for rats and should be considered exploratory, as no specific Ad26.CoV2-S dose has been validated for Wistar rats. The vaccine is produced using the PER.C6® cell line, and its potency is expressed in viral particles or infectious units [14,15]. The animals were divided as follows:

- Batch 1: Distilled water 10 ml/kg, non-immunized;
- Batch 2: Immu-C® 1 ml/100 g (pretreatment) + immunization;
- Batch 3: Garcinia kola 200 mg/kg (pretreatment) + immunization;
- Batch 4: Zingiber officinale 200 mg/kg (pretreatment) + immunization;
- Batch 5: Vaccinated control (Ad26.CoV2-S alone, without pretreatment).

This experimental setup was designed to allow the evaluation of biochemical and histopathological parameters in a pretreatment model using plant-based agents followed by vaccine immunization.

Serum biochemical parameter measurement

Blood samples were collected from the retro-orbital sinus in dry and EDTA tubes, then centrifuged at 3,000 rpm for 15 minutes to obtain serum. Serum creatinine and transaminase activities (AST and ALT) were measured using commercial kits according to the manufacturers' recommendations. Spectrophotometric readings were taken at 490 nm and 505 nm, respectively.

Pathological anatomy

Animals were anesthetized with ethyl ether and then sacrificed for histopathological examination. A systematic necropsy was performed on the liver, lungs, and spleen. The tissues were processed according to

standard histological steps, including fixation in 10% formalin, paraffin embedding, microtomy, and hematoxylin and eosin staining. Analysis was based on microscopic examination of the sections, followed by validation, report writing, and archiving of the results.

Statistical analyses

Results are expressed as means ± standard deviations. Statistical analysis was performed using ANOVA followed by Dunnett's test. Tests were conducted using SPSS version 20 and Excel 2019 (Microsoft). The significance level was set at a p-value < 0.05.

RESULTS

Effects of phytotherapeutic preconditioning on serum biochemical parameters

The effects of phytotherapeutic preconditioning on serum biochemical parameters (ALT, AST, and creatinine) were evaluated. The corresponding results are presented in Tables I to III.

Effect of immunization on serum biochemical parameters

The effects of immunization on serum biochemical parameters were evaluated by measuring transaminase activities (ALT and AST) and creatinine. The results obtained after the first and second immunizations are presented in Tables IV to VI.

Observation after immunization

The study population consisted exclusively of male Wistar rats. Two deaths were observed during the experiment, both occurring in group 5 (vaccinated control).

Anatomical pathology

The study of anatomical pathology allowed us to recognize abnormalities in the cells and tissues of an organism, called lesions, in other words, morphological alterations. This activity was carried out following the data obtained after observing male Wistar rats immunized with the Janssen Ad26.CoV2-S vaccine. Microscopy revealed various data to us.

DISCUSSION

The Ad26.CoV2-S vaccine is a recombinant non-replicating adenoviral vector vaccine developed to induce an immune response against the SARS-CoV-2 spike protein. Its widespread use during the COVID-19 pandemic demonstrated its efficacy in preventing severe forms of the disease [16-24]. However, as with any biological product, preclinical evaluation of its safety profile remains essential to better understand the biological responses that may occur after immunization. The present study aimed to evaluate the biochemical and histopathological changes observed in Wistar rats after immunization with the Ad26.CoV2-S vaccine in a phytotherapeutic preconditioning model. Analysis of biochemical parameters revealed variations in serum transaminase activities after preconditioning and then after the different phases of immunization [16,17,18]. The observed increases in ALT and AST concentrations in several groups after preconditioning suggest the existence of transient hepatic biological changes [7,11,17,18]. However, the magnitude of these variations differs between groups and is accompanied by sometimes significant dispersion of individual values, particularly for certain batches pretreated with plant extracts [9,11,18-23]. These observations therefore do not allow us to conclude that there is specific liver damage but indicate the need to interpret these changes within their overall experimental context [6,11,18]. After immunization, a decrease in serum ALT and AST activities is observed between the first and second vaccinations in the majority of groups [13,15,20]. This change could reflect a gradual adaptation of the body to the immune stimulation induced by the vaccine or the transient nature of the metabolic changes observed after the first antigenic exposure [13,20]. However, the underlying mechanisms cannot be determined based solely on the parameters studied. The results concerning creatinine, on the other hand, show a relative stability of serum concentrations during the experiment [6,11,19]. The absence of statistically significant variation between the different observation periods suggests the absence of major disruption of renal function under the conditions of this study [6,11,19]. This observation appears consistent with the overall maintenance of renal functional integrity in immunized animals [9,11,19]. In addition to the biochemical data, histopathological observations revealed several tissue changes, primarily in the lungs [10,11,21]. Histological sections highlight the presence of intra-alveolar hemorrhagic suffusions, red blood cells within the alveolar lumen, thickening of the interalveolar walls, and congested vessels [10,21]. These lesions are consistent with a pulmonary congestive and hemorrhagic process associated with increased permeability of the alveolar-capillary barrier [10,13,21]. From a pathophysiological standpoint, several mechanisms can be considered. Immune system activation induced by immunization may be

Table I: Effects of phytotherapeutic preconditioning on alanine aminotransferase levels.

Lots	Doses	ALAT		P-value
		Before treatment	After treatment	
ED	10 ml/kg	30.19 ± 10.76	40.17 ± 5.12	0.103
Imu-C	1 ml/100g	28.40 ± 5.68	48.82 ± 4.04	0.000
GK	200 mg/kg	36.25 ± 15.36	67.66 ± 42.41	0.317
ZO	200 mg/kg	40.88 ± 19.03	55.42 ± 16.89	0.108
CNV	2.5 × 10^9 vp/rat	28.52 ± 7.29	52.06 ± 7.92	0.035

Results are expressed as mean ± standard deviation. The deviation represents the difference between two means, accompanied by a standard deviation. (*) $p < 0.05$; (**) $p < 0.001$; (***) $p < 0.0001$; NS: Not significant by Dunnett's test. ED: Distilled water; Imu-C: Immu-C®; GK: Garcinia kola Heckel; ZO: Zingiber officinale Roscoe; CNV: Unvaccinated control.

Table II: Effects of phytotherapeutic preconditioning on aspartate aminotransferase levels.

Lots	Doses	AST		P-value
		Before treatment	After treatment	
ED	10 ml/kg	65.63 ± 58.98	111.89 ± 14.72	0.264
Imu-C	1 ml/100g	47.10 ± 17.25	131.37 ± 21.15	0.011
GK	200 mg/kg	42.00 ± 12.83	152.25 ± 28.24	0.008
ZO	200 mg/kg	38.21 ± 14.98	139.40 ± 30.99	0.007
CNV	2.5 × 10^9 vp/rat	96.94 ± 4.85	138.52 ± 15.50	0.015

Results are expressed as mean ± standard deviation. The deviation represents the difference between two means, accompanied by a standard deviation. (*) $p < 0.05$; (**) $p < 0.001$; (***) $p < 0.0001$; NS: Not significant by Dunnett's test. ED: Distilled water; Imu-C: Immu-C®; GK: Garcinia kola Heckel; ZO: Zingiber officinale Roscoe; CNV: Unvaccinated control.

accompanied by a transient release of inflammatory mediators capable of altering vascular permeability and promoting local congestive phenomena [13,14,20]. In this context, the observed pulmonary alterations could correspond to a tissue inflammatory response secondary to immune stimulation [13,14,20]. Examination of the liver shows congestion of the central lobe vein without major morphological alterations of the hepatocytes. The absence of cell ballooning, the preservation of the hepatic trabecular architecture, and the regularity of the nuclei suggest an overall preservation of the histological organization of the liver parenchyma [9,11,23]. These observations appear consistent with the moderate variations in liver biochemical parameters recorded during the study [6,11,17,18]. In the spleen, the clear distinction between white and red pulp, as well as the presence of a well-defined lymphoid follicle, demonstrates the maintenance of the organ's overall architecture [10,14,23]. The abundance of lymphoid cells observed in the white pulp could be consistent with immune activation following immunization, but a definitive functional interpretation is not possible without further immunohistochemical analyses [13,14,18,23]. Two deaths were recorded during the study, both in Group 5, the vaccinated control group receiving Ad26.CoV2-S without plant pretreatment. The first death occurred 48 hours after the second immunization and the second at 72 hours, resulting in a mortality rate of 50% (2/4) in this group. No deaths were observed in the

Table III: Effects of phytotherapeutic preconditioning on creatinine levels

Lots	Doses	CREAT		P-value
		Before treatment	After treatment	
ED	10 ml/kg	1.18 ± 1.93	0.20 ± 0.33	0.310
Imu-C	1 ml/100g	0.34 ± 0.29	0.41 ± 0.56	0.825
GK	200 mg/kg	1.70 ± 3.08	0.17 ± 0.19	0.399
ZO	200 mg/kg	0.64 ± 0.32	0.21 ± 0.15	0.086
CNV	2.5 × 10^9 vp/rat	0.25 ± 0.12	0.54 ± 0.37	0.301

Results are expressed as mean ± standard deviation. The deviation represents the difference between two means, accompanied by a standard deviation. (*) $p < 0.05$; (**) $p < 0.001$; (***) $p < 0.0001$; NS: Not significant by Dunnett's test. ED: Distilled water; Imu-C: Immu-C®; GK: Garcinia kola Heckel; ZO: Zingiber officinale Roscoe; CNV: Unvaccinated control.

Table IV: Effect of immunization on Alanine Aminotransferase levels

Lots	Doses	ALAT		P-value
		1st Vaccination	2nd Vaccination	
ED	10 ml/kg	43.59 ± 17.52	19.10 ± 10.76	0.033
Imu-C	1 ml/100g	54.00 ± 9.04	33.60 ± 3.45	0.034
GK	200 mg/kg	43.17 ± 14.25	28.00 ± 7.66	0.258
ZO	200 mg/kg	66.39 ± 22.13	31.07 ± 10.61	0.092
CV	2.5 × 10^9 vp/rat	54.37 ± 7.53	26.53 ± 7.61	0.014

Results are expressed as mean ± standard deviation. The deviation represents the difference between two means, accompanied by a standard deviation. (*) $p < 0.05$; (**) $p < 0.001$; (***) $p < 0.0001$; NS: Not significant by Dunnett's test. ED: Distilled water; Imu-C: Immu-C®; GK: Garcinia kola Heckel; ZO: Zingiber officinale Roscoe; CV: Vaccinated control.

Table V: Effect of immunization on Aspartate Aminotransferase levels.

Lots	Doses	AST		P-value
		1st Vaccination	2nd Vaccination	
ED	10 ml/kg	165.20 ± 89.91	28.87 ± 9.07	0.047
Imu-C	1 ml/100g	140.12 ± 32.90	35.39 ± 16.14	0.013
GK	200 mg/kg	156.20 ± 35.63	40.98 ± 11.73	0.002
ZO	200 mg/kg	303.35 ± 127.45	52.07 ± 22.71	0.036
CV	2.5 × 10^9 vp/rat	173.94 ± 20.51	83.80 ± 9.78	0.011

Results are expressed as mean ± standard deviation. The deviation represents the difference between two means, accompanied by a standard deviation. (*) $p < 0.05$; (**) $p < 0.001$; (***) $p < 0.0001$; NS: Not significant by Dunnett's test. ED: Distilled water; Imu-C: Immu-C®; GK: Garcinia kola Heckel; ZO: Zingiber officinale Roscoe; CV: Vaccinated control.

Table VI: Effect of immunization on creatinine levels.

Lots	Doses	CREAT		P-value
		1st Vaccination	2nd Vaccination	
ED	10 ml/kg	0.19 ± 0.01	0.15 ± 0.20	0.555
Imu-C	1 ml/100g	0.25 ± 0.24	0.06 ± 0.05	0.261
GK	200 mg/kg	0.53 ± 0.55	0.40 ± 0.45	0.508
ZO	200 mg/kg	0.22 ± 0.11	0.14 ± 0.09	0.321
CV	2.5 × 10^9 vp/rat	0.23 ± 0.07	0.32 ± 0.22	0.436

Results are expressed as mean ± standard deviation. The deviation represents the difference between two means, accompanied by a standard deviation. (*) $p < 0.05$; (**) $p < 0.001$; (***) $p < 0.0001$; NS: Not significant by Dunnett's test. ED: Distilled water; Imu-C: Immu-C®; GK: Garcinia kola Heckel; ZO: Zingiber officinale Roscoe; CV: Vaccinated control.

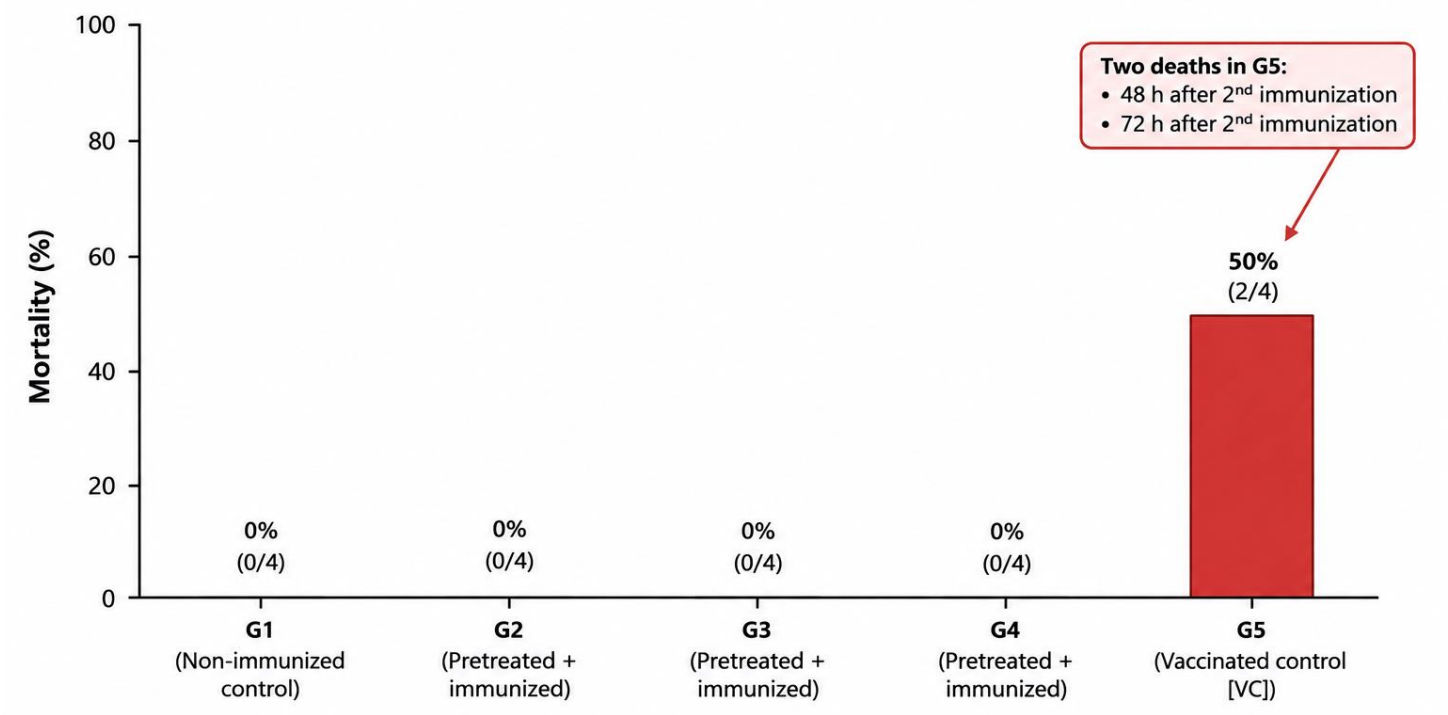


Figure 1: Mortality observed in each experimental group.

non-immunized control group or in any of the plant-pretreated and immunized groups. This mortality pattern represents an observation within the experimental setting that warrants further investigation, particularly to clarify the potential factors associated with these events [12,13,18]. Overall, in this experi-

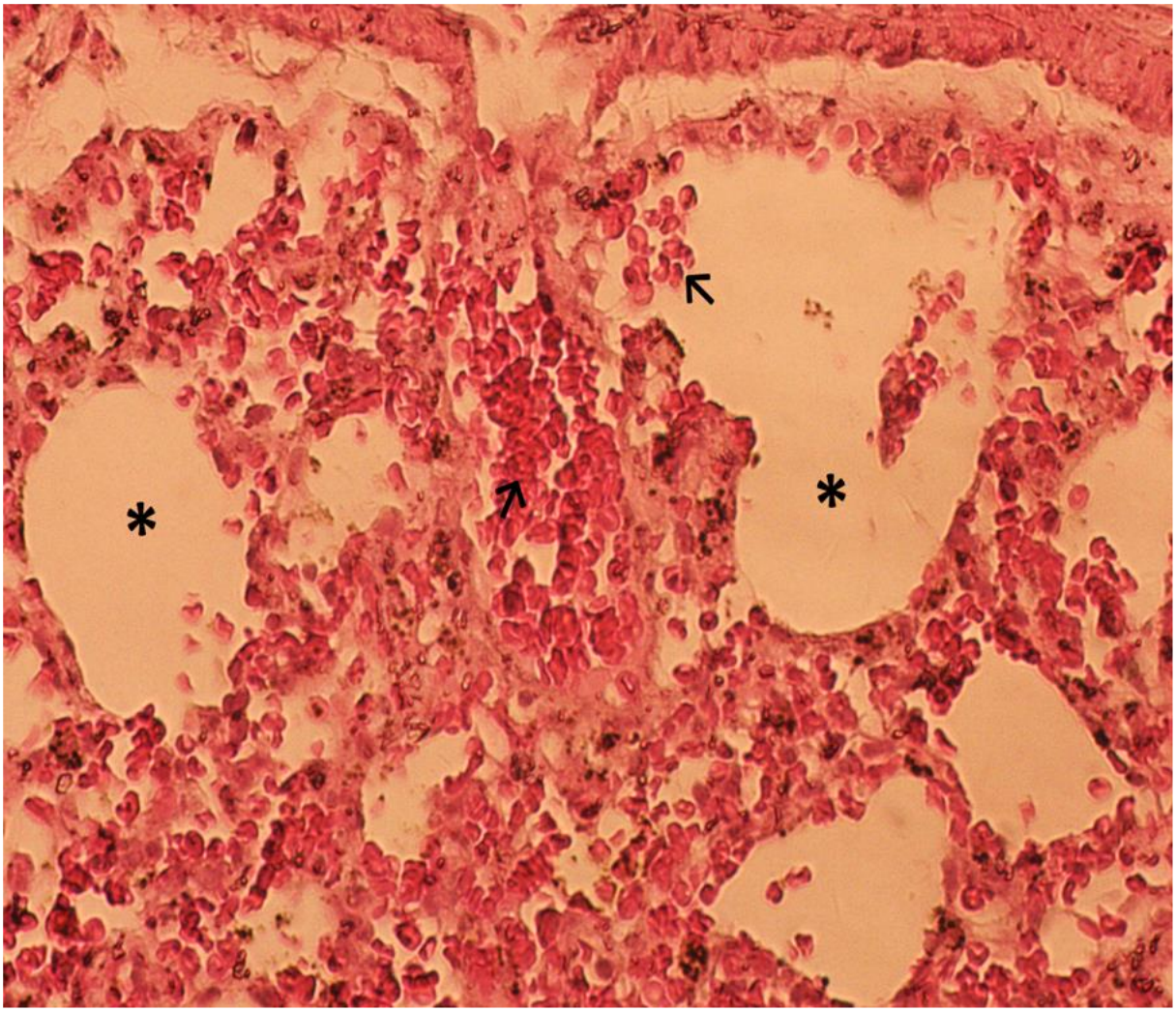


Figure 2: Micrograph of the pulmonary alveoli of an immunized male Wistar rat

Figure 2, at medium magnification, shows the presence of hemorrhagic suffusion (→) in the alveolar lumen and in the alveolar septa. This indicates congestive and hemorrhagic inflammation with breach of the air-blood barrier. (Staining: Hematoxylin-Eosin).

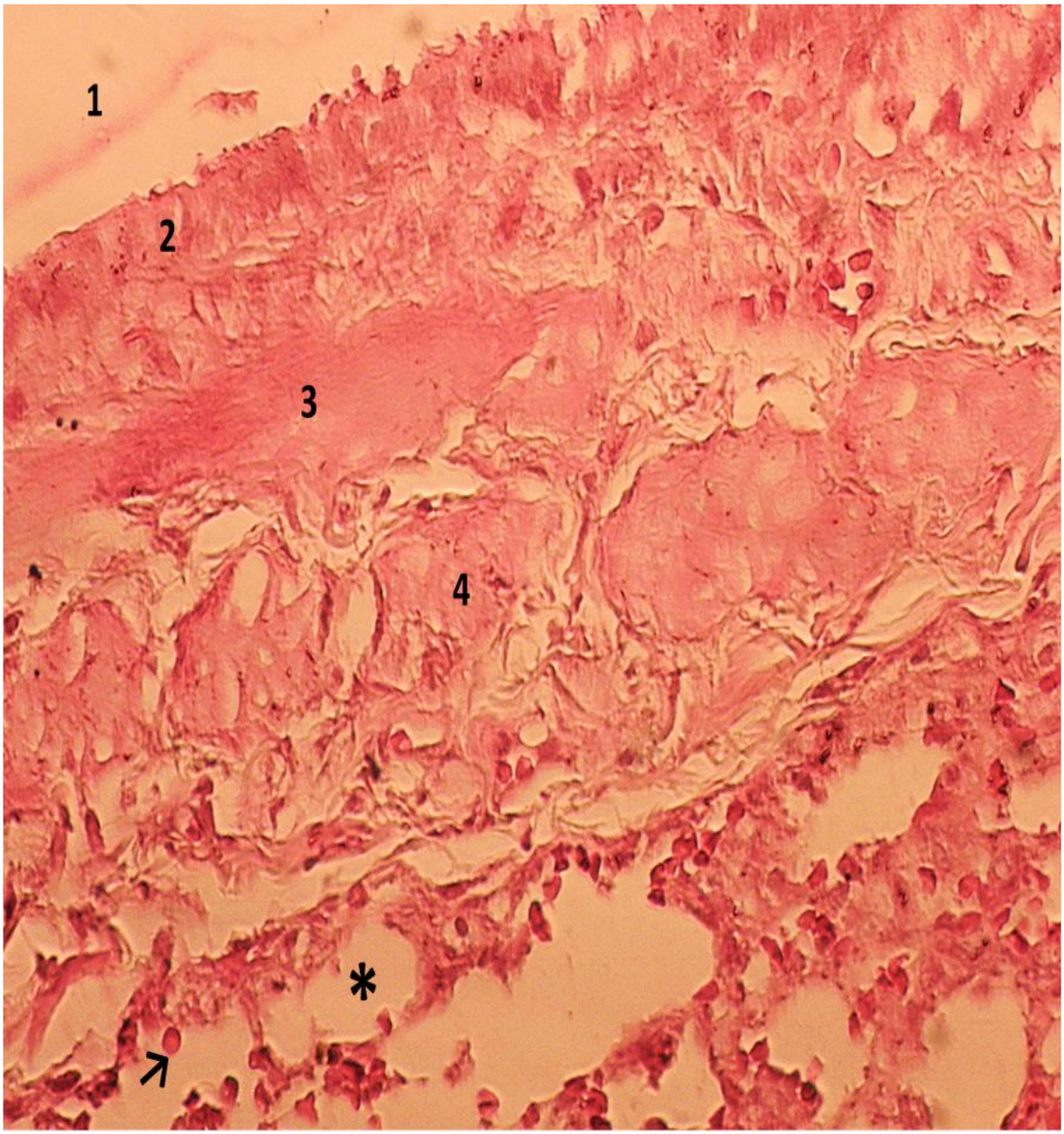


Figure 3: Photomicrograph of the lungs of an immunized male Wistar rat.

Figure 3, at low magnification, shows the presence of red blood cells (→) in the lumen of the alveoli (*). It also shows: the lumen of a bronchus (1), the lining of the bronchus (2), Resseinssen's muscle (3), and cartilaginous clusters (4). (Staining: Hematoxylin-Eosin)

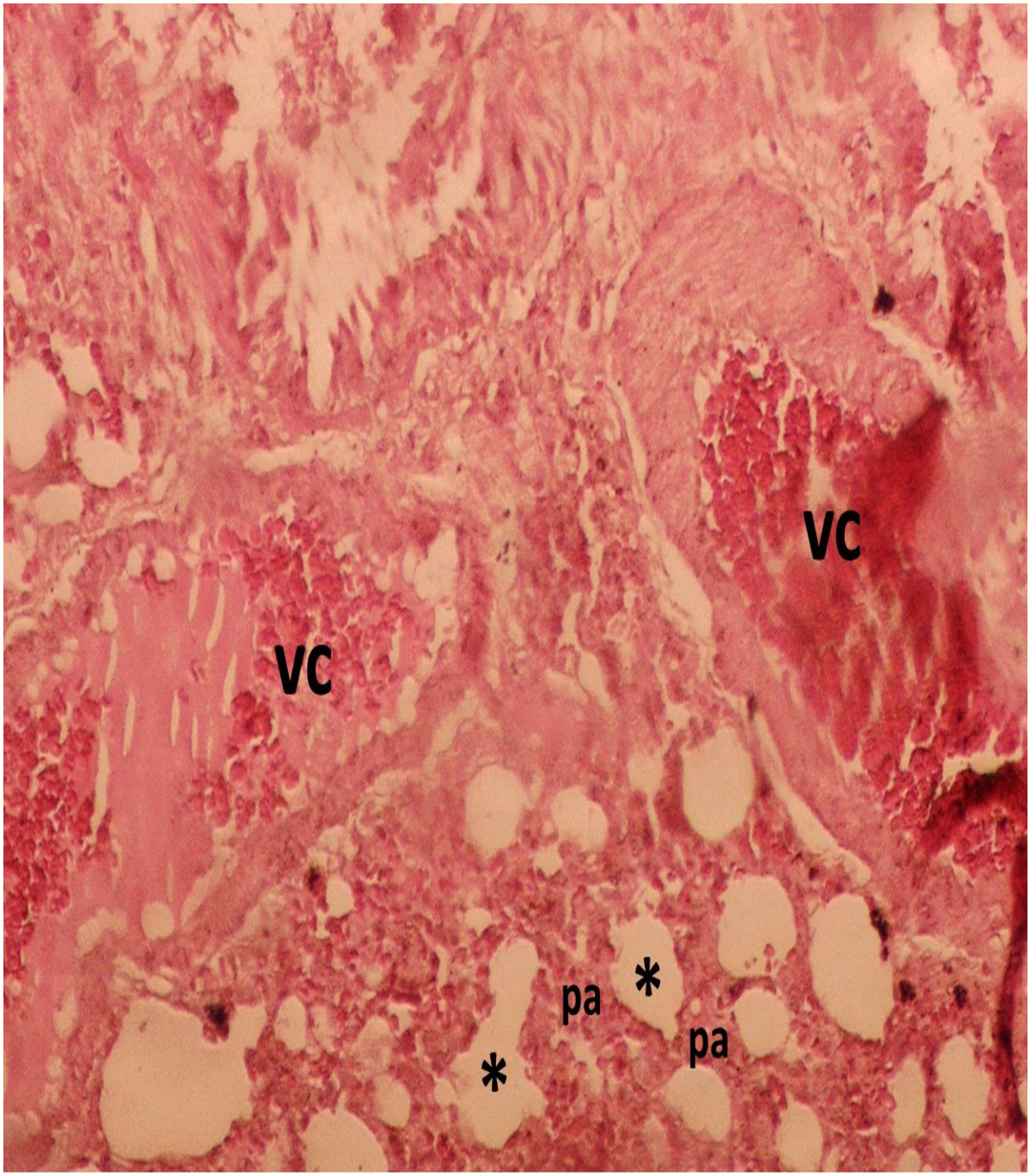


Figure 4: Photomicrograph of the effect of immunization on the lungs of a male Wistar rat

Figure 4, at medium magnification, shows congested vessels [vc], thickening of the interalveolar walls (pa), and the alveolar lumen. (Staining: Hematoxylin-Eosin).

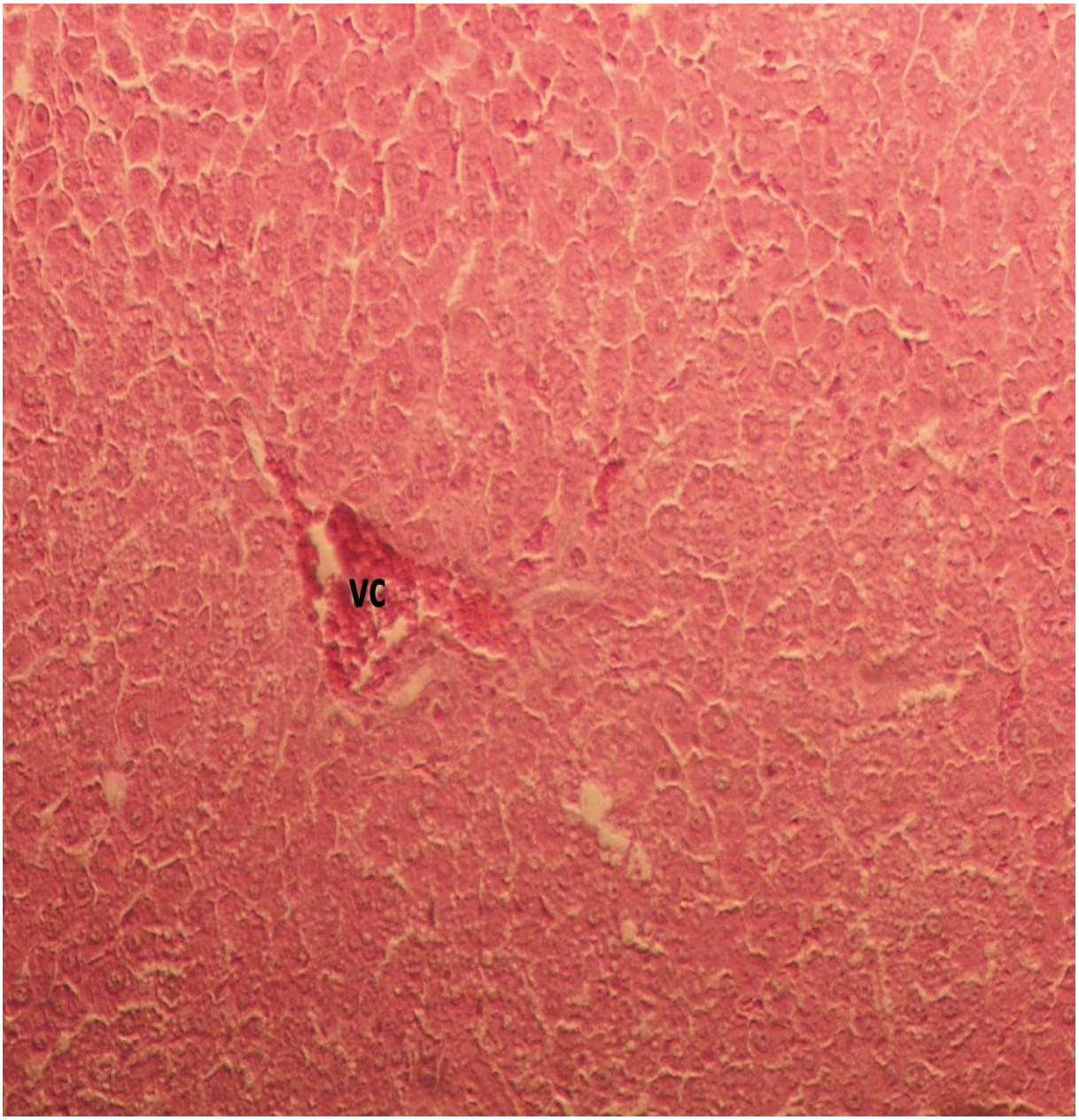


Figure 5: Micrograph of the effect of immunization on the liver of a male Wistar rat.

The low-magnification microscopic view reveals congestion of the centrilobular vein (VC), an arrangement of hepatocytes in single-cell trabeculae without ballooning, homogeneity of their cytoplasm, and regularity of their nuclei. (Staining: Hematoxylin and Eosin).

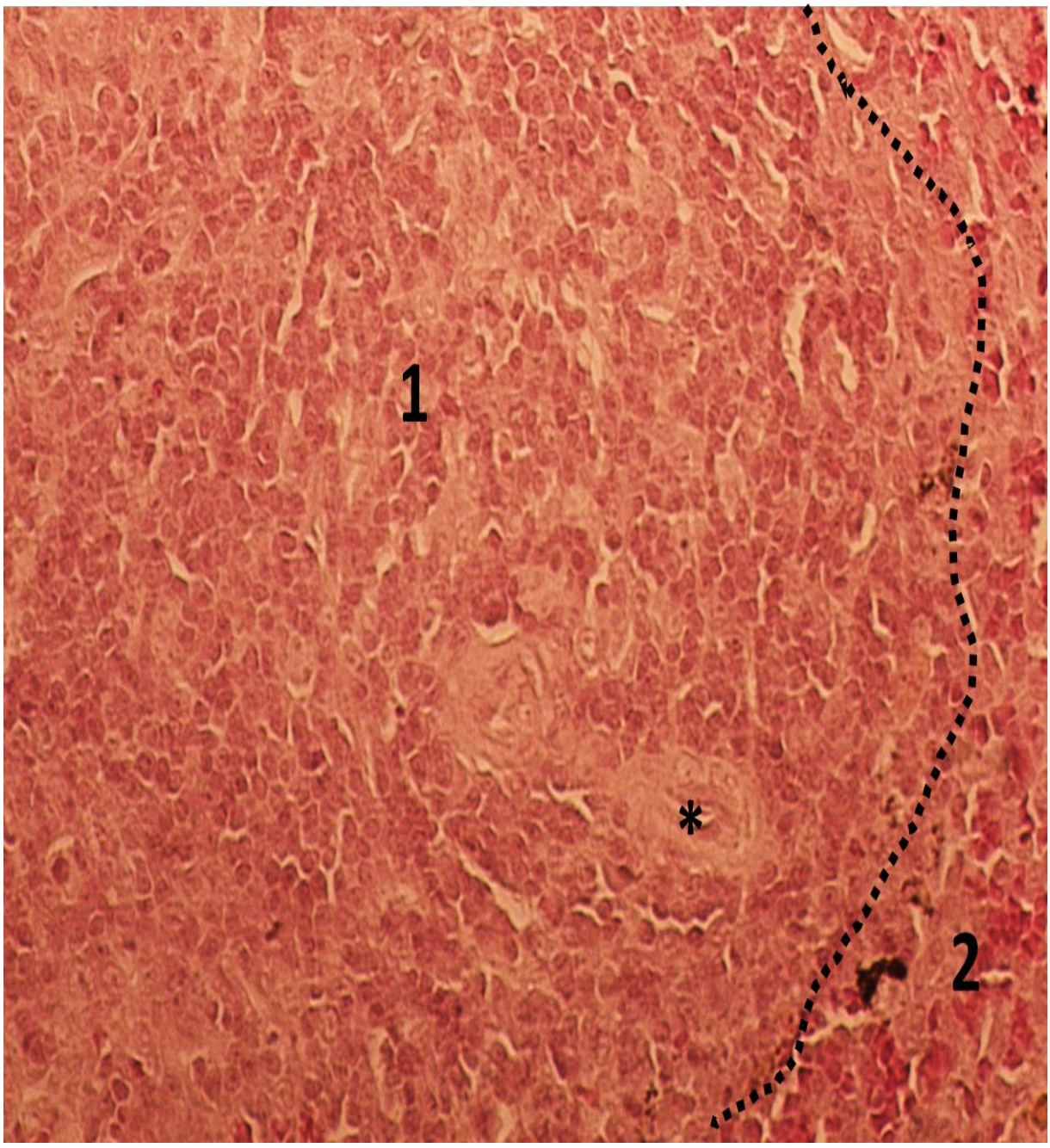


Figure 6: Photomicrograph of the white pulp of the spleen of a male Wistar rat.

Figure 6, at medium magnification, shows the splenic follicle composed of lymphoid cells (lymphocytes and plasma cells), the lymphoid follicle or white pulp (1), red pulp (2), the boundary between the two pulps (…), and central follicular vessels. (Staining: Hematoxylin and Eosin)

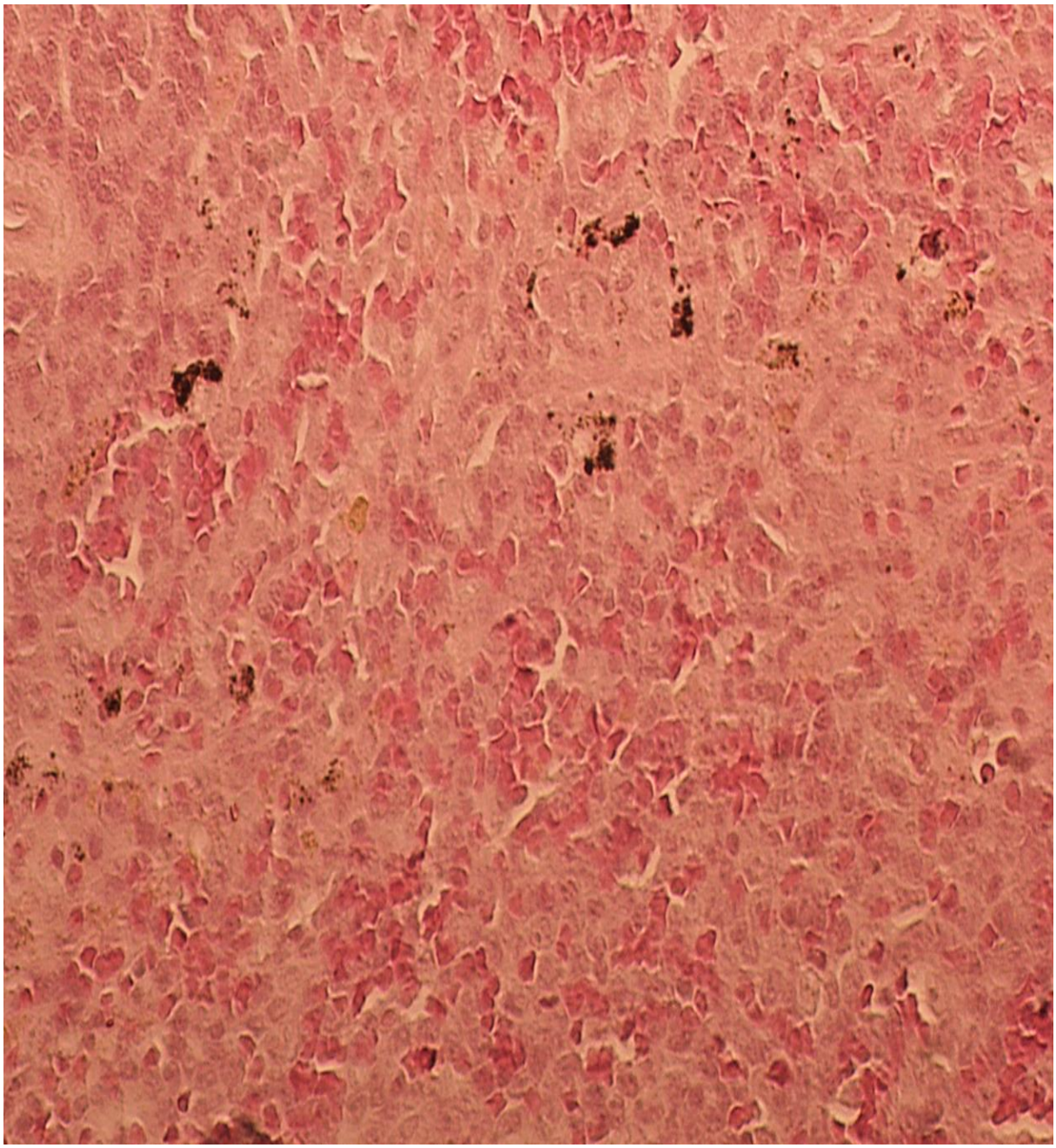


Figure 7: Micrograph of the red pulp of the spleen of a male Wistar rat.

The low-magnification microscopic view in Figure 7 reveals that red blood cells are present in moderate quantities in the connective tissue. (Staining: Hematoxylin and Eosin).

mental model, the Ad26.CoV2-S vaccine is associated with biological changes dominated by inflammatory lung damage, while renal and hepatic functions appear relatively preserved [12,15,24]. The small sample size, the lack of additional molecular analyses, and the exploratory nature of the experimental model limit the scope of interpretations and define the framework for the scientific interpretation of the results [6,7,18,22].

CONCLUSION

In Wistar rats immunized with Ad26.CoV2-S in a phytotherapeutic preconditioning setting, transaminase levels fluctuated without a stable trend, while creatinine remained largely unchanged. Histopathological lesions primarily affected the lungs (congestion and alveolar hemorrhage), with the liver and spleen generally spared. Two deaths were observed in the vaccinated control group. Overall, these findings suggest moderate biological changes dominated by pulmonary involvement, requiring further investigation.

REFERENCES

1.Cevik M, Bamford CGG, Ho A. COVID-19 pandemic: a focused review for clinicians. Clin Microbiol Infect. 2020 Jul;26(7):842-847. doi:10.1016/j.cmi.2020.04.023. PMID:32344166; PMCID:PMC7182753.

2.Mohammed I, Nauman A, Paul P, Ganesan S, Chen KH, Jalil SMS, et al. The efficacy and effectiveness of the COVID-19 vaccines in reducing infection, severity, hospitalization, and mortality: a systematic review. Hum Vaccin Immunother. 2022;18(1). doi:10.1080/21645515.2022.2027160.

3.Le Gars M, Hendriks J, Sadoff J, et al. Immunogenicity and efficacy of Ad26.COV2.S: An adenoviral vector-based COVID-19 vaccine. Immunol Rev. 2022;310:47-60. doi:10.1111/imr.13088.

4.Hardt K, Vandebosch A, Sadoff J, et al. Efficacy, safety, and immunogenicity of a booster regimen of Ad26.COV2.S vaccine against COVID-19 (ENSEMBLE2): results from a randomized, double-blind, placebo-controlled phase 3 trial. Lancet Infect Dis. 2022;22:1703-1715. doi:10.1016/S1473-3099(22)00506-0.

5.Burke PF, Masters D, Massey G. Enablers and barriers to COVID-19 vaccine uptake: an international study of perceptions and intentions. Vaccine. 2021;39(36):5116-5128. doi:10.1016/j.vaccine.2021.07.056.

6.Baylor NW. The regulatory evaluation of vaccines for human use. In: Methods in Molecular Biology. 2016;1404:773-787. doi:10.1007/978-1-4939-3389-1_51.

7.Doroud D, Daneshi M, Kazemi-Lomedash F, Eftekhari Z. Comprehensive review of preclinical evaluation strategies for COVID-19 vaccine candidates: assessing immunogenicity, toxicology, and safety profiles. Iran J Microbiol. 2025;17(1):1-18. doi:10.18502/ijm.v17i1.17796.

8.Lai LY, Arshad F, Areia C, et al. Current approaches to vaccine safety using observational data: a rationale for the EUMAEUS study design. Front Pharmacol. 2022;13:837632. doi:10.3389/fphar.2022.837632.

9.Sellers RS, Morton D, Michael B, et al. Society of Toxicologic Pathology position paper: organ weight recommendations for toxicology studies. Toxicol Pathol. 2007;35(5):751-755. doi:10.1080/01926230701595300.

10.Iannaccone PM, Jacob HJ. Rats! Dis Model Mech. 2009;2(5-6):206-210. doi:10.1242/dmm.002733.

11.Tripathi NK, Ramaiah L, Arndt T, et al. Opinion on qualitative severity descriptors to express magnitude of changes in clinical pathology endpoints in nonclinical toxicity studies. Toxicol Pathol. 2025;53(6):561-570. doi:10.1177/01926233251341271.

12.Sadoff J, Gray G, Vandebosch A, et al. Safety and efficacy of single-dose Ad26.COV2.S vaccine against Covid-19. N Engl J Med. 2021;384(23):2187-2201. doi:10.1056/NEJMoa2101544.

13.Custers J, Kim D, Leyssen M, et al. Vaccines based on replication-incompetent Ad26 viral vectors: standardized template with key considerations for a risk/benefit assessment. Vaccine. 2021;39(22):3081-3101. doi:10.1016/j.vaccine.2020.09.018.

14.Bos R, Rutten L, van der Lubbe JEM, et al. Ad26 vector-based COVID-19 vaccine encoding a prefusion-stabilized SARS-CoV-2 spike immunogen induces potent humoral and cellular immune responses. NPJ Vaccines. 2020;5:91. doi:10.1038/s41541-020-00243-x.

15.Sadoff J, Le Gars M, Shukarev G, et al. Interim results of a phase 1–2a trial of Ad26.COV2.S COVID-19 vaccine. N Engl J Med. 2021;384(19):1824-1835. doi:10.1056/NEJMoa2034201.

16.Cavagnaro J, Sims J. ICH S6 preclinical safety evaluation of biotechnology-derived pharmaceuticals. In: Müller L, editor. Global approach in safety testing. New York: Springer; 2013. p. 215-242. doi:10.1007/978-1-4614-5950-7_10.

17.Ozer J, Ratner M, Shaw M, Bailey W, Schomaker S. The current state of serum biomarkers of hepatotoxicity. Toxicology. 2008;245(3):194-205. doi:10.1016/j.tox.2007.11.021.

18. Park SJ, Jang MS, Lim KH, Seo JW, Im WJ, Han KH, Kim SE, Jang E, Park D, Kim YB. Preclinical evaluation of general toxicity and safety pharmacology of a receptor-binding domain-based COVID-19 subunit vaccine in various animal models. Arch Toxicol. 2023;97(9):2429-2440. doi:10.1007/s00204-023-03549-6.

19.Ferguson MA, Waikar SS. Established and emerging markers of kidney function. Clin Chem. 2012;58(4):680-689. doi:10.1373/clinchem.2011.167494.

20.Tregoning JS, Russell RF, Kinnear E. Adjuvanted and vectored vaccines: immunological mechanisms of reactogenicity. Nat Rev Immunol. 2021;21:626-636. doi:10.1038/s41577-021-00592-1.

21.Wazny V, Siau A, Wu KX, Cheung C. Vascular underpinning of COVID-19. Open Biol. 2020;10(8):200208. doi:10.1098/rsob.200208.

22.Smith JR, Bolton ER, Dwinell MR. The Rat: A Model Used in Biomedical Research. Methods Mol Biol. 2019;2018:1-41. doi: 10.1007/978-1-4939-9581-3_1.

23.Haschek WM, Rousseaux CG, Wallig MA, editors. Haschek and Rousseaux's handbook of toxicologic pathology. 3rd ed. London: Academic Press; 2013. 3 vols. doi:10.1016/C2010-1-67850-9.

24.Caramaschi S, Kapp ME, Miller SE, Eisenberg R, Johnson J, Epperly G, Maiorana A, Silvestri G, Giannico GA. Histopathological findings and clinicopathologic correlation in COVID-19: a systematic review. Mod Pathol. 2021;34(9):1614-1633. doi:10.1038/s41379-021-00814-w.